Electronic Supplementary Material (ESI) for Journal of Materials Chemistry A.

Supplementary Information for

Renewable flexible supercapacitors based on all-lignin-based hydrogel electrolytes and nanofiber electrodes

Jeong Hee Park, [‡a] Harpalsinh Hardevsinh Rana, [‡a] Jun Young Lee*[a] and Ho Seok Park *[abc]

[a] *School of Chemical Engineering, College of Engineering, Sungkyunkwan University, 2066, Seobu-ro, Jangan-gu, Suwon-si, Gyeonggi-do 440-746, Republic of Korea*

[b] *Department of Health Sciences and Technology, Samsung Advanced Institute for Health Sciences and Technology (SAIHST), Sungkyunkwan University, 2066, Seobu-ro, Jangan-gu, Suwon-si, Gyeonggi-do 440-746, Republic of Korea*

[c] *SKKU Advanced Institute of Nano Technology (SAINT), Sungkyunkwan University, 2066, Seobu-ro, Jangan-gu, Suwon-si, Gyeonggi-do 440-746, Republic of Korea*

‡These authors are equally contributed to work

* To whom correspondence should be addressed.

E-mail: phs0727@skku.edu, jylee7@skku.edu

Characterizations

Solid-state ^{13}C NMR and liquid ^{13}C NMR analyses were carried out using 400 MHz Bruker solid-state NMR and 500 MHz Bruker FT-NMR at KBSI Seoul Western Center, respectively. Thermogravimetric analysis (TGA) and differential thermal analysis (DTA) were conducted by Seiko Exstar 6000 in the temperature range of 25 - 600 ^{o}C with a heating rate of 10 ^{o}C min-1 under a nitrogen atmosphere. The morphology of all samples was studied with field emission-scanning electron microscope (FE-SEM, LEO SUPRA 55, 15kV) and transmission electron microscope (TEM, EM912 Omega, 120 kV). The structural characterization were carried out by an X-ray diffraction (XRD) using D8 Advance powder diffraction (wavelength = 1.5406 Å) and Raman spectroscopy using in Via Raman microscope. N_2 adsorption-desorption isotherms were obtained by a Brunauer-Emmett-Teller apparatus (BET, BELSORP-mini II). The specific surface areas of the materials were calculated from BET method and the pore size distributions were derived by the BJH mode.

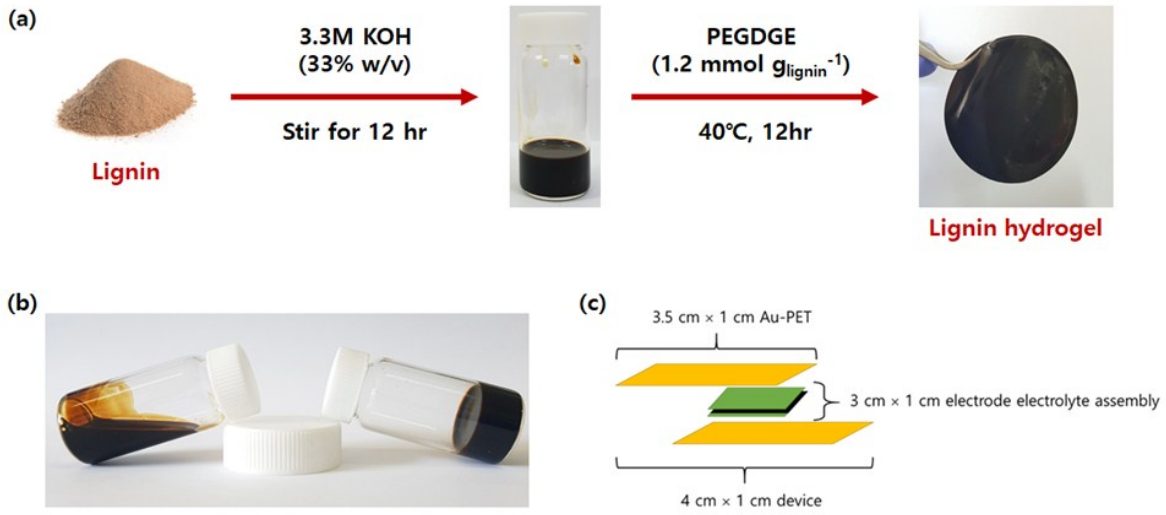

Figure S1. (a) Synthetic scheme of lignin hydrogel, (b) State of reaction mixture before and after crosslinking, (c) schematic illustration of device geometry.

For electrochemical characterization, we have used device having 1cm x 1 cm electrode-electrolyte assembly, which was then sandwiched between two 1.5 cm x 1 cm Au-coated PETs (0.5 cm extra length for connection, so final device geometry is 2cm x 2 cm). Similarly, for tandem configuration and bending test, 3 cm x 1 cm electrode-electrolyte assembly was sandwiched between two 3.5 cm x 1 cm Au-coated PETs and the final device dimension is 4 cm x 1 cm, which can be very easily bent to different angles.

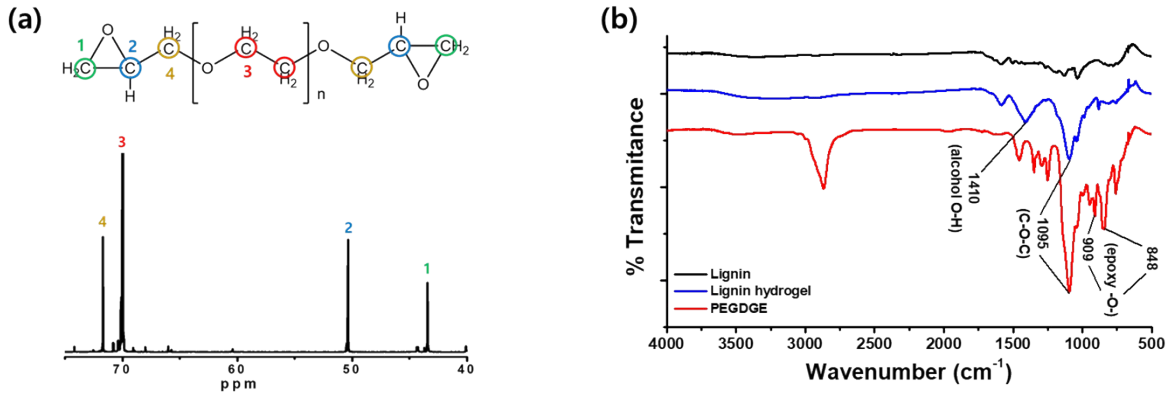

Figure S2. (a) ^{13}C NMR spectrum of PEGDGE. (b) FT-IR spectra of the lignin, lignin hydrogel, and PEGDGE.

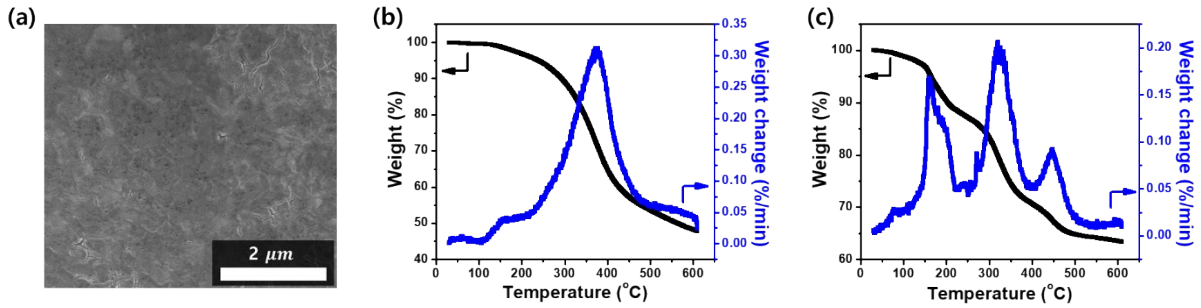

Figure S3. (a) SEM image of lignin hydrogel before swelling. (b, c) TGA and DTG curves of the pristine lignin and lignin hydrogel.

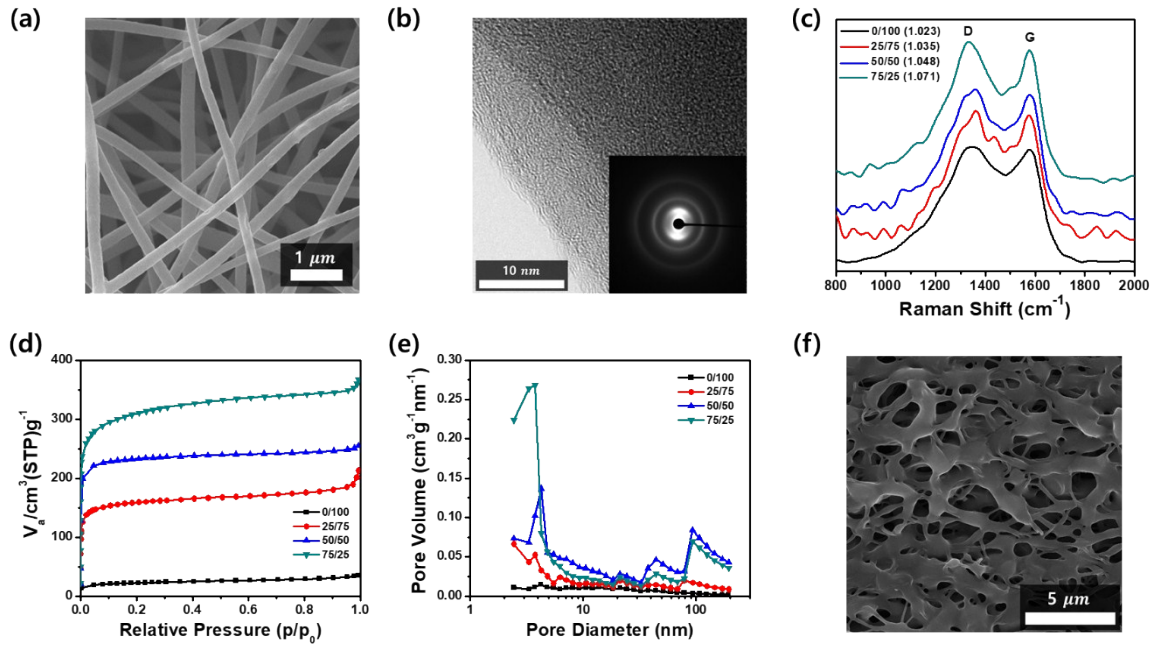

Figure S4. (a, b) SEM and HR-TEM images of pristine PAN ECNFs. (c) Raman spectra of for different lignin/PAN ECNFs. (d, e) N_2 adsorption isotherms and pore size distribution plots for different ECNFs. (f) SEM image of lignin/PAN (75/25) ECNFs.

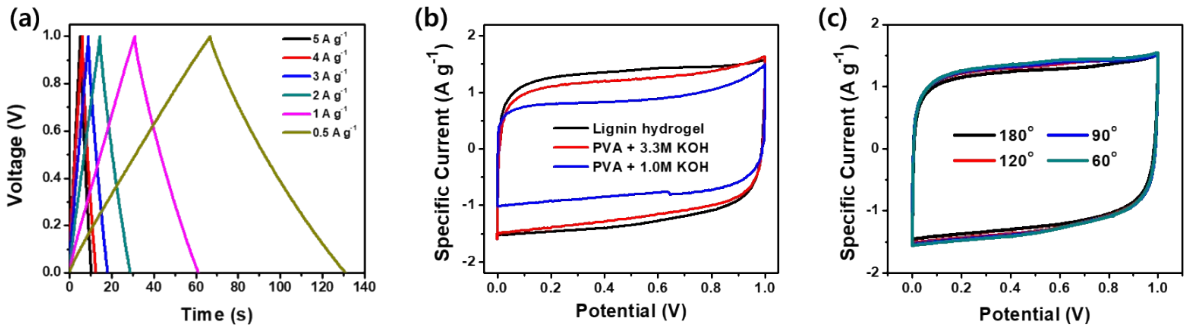

Figure S5. (a) GCD profiles of lignin-based SCs at current densities from 0.5 to 5 A g^{-1}. (b) CV curves of the lignin-based SC and two SCs using PVA/KOH (1.0 and 3.3 M) hydrogel at 50 mV s^{-1}. (c) CV curves of lignin-based SCs at bending angles of 60°, 90°, 120°, and 180° at 50 mV s^{-1}.

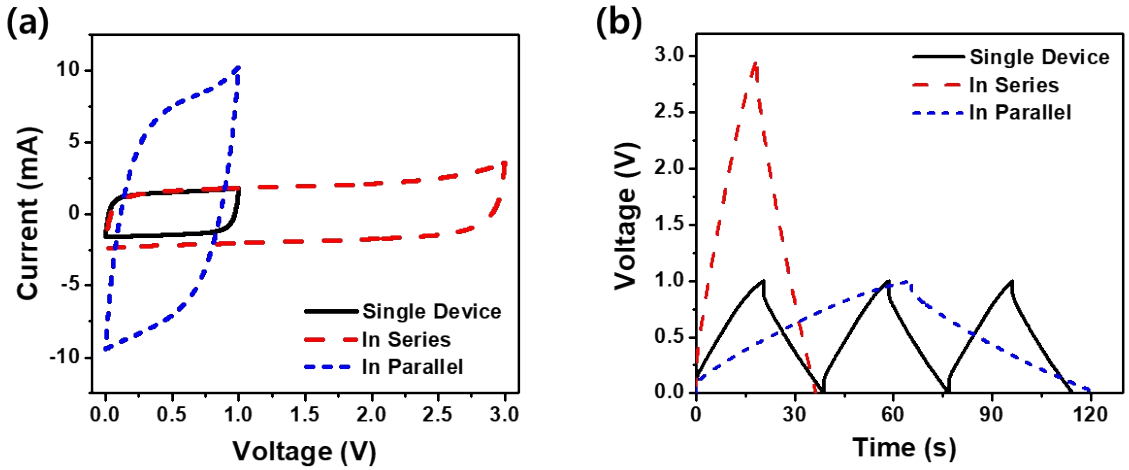

Figure S6. (a, b) CV curves at a scan rate of 50 mV s^{-1} and GCD profiles at a constant current of 5 mA for the single and tandem configuration of lignin-based SCs.

Table S1. Specific surface area, total pore volume and mean pore diameter comparison analysis based on BET method for only PAN, lignin/PAN (25/75), (50/50) and (75:25) ECNFs, respectively.

Sample	PAN	25:75	50:50	75:25
Specific surface area [$m^2 g^{-1}$]	80.0	607.5	918.5	1176.0
Total pore volume [$cm^3 g^{-1}$]	0.054	0.329	0.394	0.568
Mean pore diameter [nm]	2.681	2.170	1.715	1.930

Table S2. Elemental compositions of different lignin/PAN ECNFs analyzed by XPS analysis.

Sample (Lignin/PAN)	Atomic % of C	Atomic % of O	Atomic % of S
Lignin (0/100)	77.68	5.5	0
Lignin (25/75)	78.58	12.13	0.28
Lignin (50/50)	79.23	16.5	0.35
C-Lignin (0/100)	87.29	7.45	0
C-Lignin (25/75)	87.33	9.95	0.13
C-Lignin (50/50)	87.89	9.83	0.23

* C - after carbonization

Table S3. Comparison of various symmetric flexible supercapacitors based on carbon freestanding electrodes and aqueous gel or liquid electrolytes.

Electrode	Electrolyte	Specific capacitance ($F\ g^{-1}$)	Capacity retention (Cycle stability)	Coulombic efficiency	Ref.
Lignin/PAN nanofiber	Lignin/KOH	129 at 0.5 A g^{-1} 108 at 5.0 A g^{-1}	95% after 10,000 cycles at 5.0 A g^{-1}	99% at 5.0 A g^{-1}	This work
3D porous graphitic biomass carbon	PVA/KOH	222 at 0.5 A g^{-1} 127 at 5.0 A g^{-1}	84% after 10,000 cycles at 5.0 A g^{-1}	N/A	[1]
N,S co-doped 3D graphene hydrogel	PVA/KOH	148 at 2.0 A g^{-1}	69% after 4,000 cycles at 2.0 A g^{-1}	N/A	[2]
CNF/PANI	PVA/H_2SO_4	201 at 0.25 A g^{-1} 100 at 4.0 A g^{-1}	80% after 6,000 cycles at 1.0 A g^{-1}	99% at 1.0 A g^{-1}	[3]
Polyuretane/ rGO/SWCNT	PVA/H_3PO_4	43 at 1.0 A g^{-1}	95% after 1,000 cycles at 1.0 A g^{-1}	N/A	[4]
$MoSe_2$/MWCNT	PVA/KOH	52 at 0.6 A g^{-1} 25 at 1.0 A g^{-1}	93% after 1,000 cycles at 100 mV s^{-1}	97% at 1.0 A g^{-1}	[5]
Porous carbon nanofiber	H_2SO_4	67 at 0.2 A g^{-1} 61 at 0.5 A g^{-1}	69% after 2,000 cycles at 1 A g^{-1}	N/A	[6]
Polypyrrole hydrogel	PVA/H_2SO_4	190 at 0.5 A g^{-1} 101 at 8.0 A g^{-1}	90% after 3,000 cycles at 1.0 A g^{-1}	N/A	[7]

References

1. Y. Gong, D. Li, C. Luo, Q. Fu and C. Pan, *Green Chem.*, 2017, **19**, 4132-4140.
2. W. Zhang, Z. Chen, X. Guo, K. Jin, Y. Wang, L. Li, Y. Zhang, Z. Wang, L. Sun and T. Zhang, *Electrochim. Acta*, 2018, **278**, 51-60.
3. F. Miao, C. Shao, X. Li, N. Lu, K. Wang, X. Zhang and Y. Liu, *Energy*, 2016, **95**, 233-241.
4. H. T. Jeong, J. F. Du, Y. R. Kim, C. J. Raj and B. C. Kim, *J. Alloys Compd.*, 2019, **777**, 67-72.
5. S. S. Karade and B. R. Sankapal, *J. Electroanal. Chem.*, 2017, **802**, 131-138.
6. Y. Liu, J. Zhou, L. Chen, P. Zhang, W. Fu, H. Zhao, Y. Ma, X. Pan, Z. Zhang and W. Han, *ACS Appl. Mater. Interfaces*, 2015, **7**, 23515-23520.
7. J. Bo, X. Luo, H. Huang, L. Li, W. Lai and X. Yu, *J. Power Sources*, 2018, **407**, 105-111.